European Surgical Research

Eur Surg Res 2020;61:143–152
DOI: 10.1159/000513335
Received: August 24, 2020
Accepted: November 20, 2020
Published online: January 28, 2021

Methods Article

Clinical Implementation of In-House Developed MR-Based Patient-Specific 3D Models of Liver Anatomy

Oleksandra V. Ivashchenko[a, b] Jasper N. Smit[a] Jasper Nijkamp[a] Leon C. ter Beek[c] Erik-Jan Rijkhorst[c] Niels F.M. Kok[a] Theo J.M. Ruers[a, d] Koert F.D. Kuhlmann[a]

[a]Department of Surgical Oncology, The Netherlands Cancer Institute – Antoni van Leeuwenhoek Hospital, Amsterdam, The Netherlands; [b]Department of Radiology, Leiden University Medical Center, Medical Physics Group, Leiden, The Netherlands; [c]Department of Medical Physics and Technology, The Netherlands Cancer Institute – Antoni van Leeuwenhoek Hospital, Amsterdam, The Netherlands; [d]Faculty of Science and Technology (TNW), Nanobiophysics Group (NBP), University of Twente, Enschede, The Netherlands

Keywords
Anatomical models · Liver surgery · 3D anatomy · Preoperative planning · Image-guided surgery

Abstract
Knowledge of patient-specific liver anatomy is key to patient safety during major hepatobiliary surgery. Three-dimensional (3D) models of patient-specific liver anatomy based on diagnostic MRI images can provide essential vascular and biliary anatomical insight during surgery. However, a method for generating these is not yet publicly available. This paper describes how these 3D models of the liver can be generated using open source software, and then subsequently integrated into a sterile surgical environment. The most common image quality aspects that degrade the quality of the 3D models as well possible ways of eliminating these are also discussed. Per patient, a single diagnostic multiphase MRI scan with hepatospecific contrast agent was used for automated segmentation of liver contour, arterial, portal, and venous anatomy, and the biliary tree. Subsequently, lesions were delineated manually. The resulting interactive 3D model could be accessed during surgery on a sterile covered tablet. Up to now, such models have been used in 335 surgical procedures. Their use simplified the surgical treatment of patients with a high number of liver metastases and contributed to the

O.V.I. and J.N.S. contributed equally to this work. Video renderings of the 3D models are added to provide insights in the anatomical situations of the cases.

Oleksandra V. Ivashchenko
Department of Radiology, Leiden University Medical Center
Medical Physics Group, K4–44
Albinusdreef 2, NL–2333 ZA Leiden (The Netherlands)
o.ivashchenko@lumc.nl

Karger

localization of vanished lesions in cases of a radiological complete response to neoadjuvant treatment. They facilitated perioperative verification of the relationship of tumors and the surrounding vascular and biliary anatomy, and eased decision-making before and during surgery.

Introduction

As a result of effective systemic treatment regimens, the development of surgical techniques, and improvements in perioperative management, the indications for the surgical treatment of liver malignancies are expanding [1]. Liver surgery can be challenging due to the anatomical complexity of the organ and interpatient anatomical variability, especially in patients with multiple bilobar or centrally located lesions in close proximity to major vessels and bile ducts, or else due to the difficulty to localize vanished lesions after systemic therapy [2]. Currently, surgeons primarily base their resection plans on the preoperative assessment of diagnostic images. If evaluation of imaging is needed during the surgery, they have to pause the procedure and reassess available imaging on a radiology station in the operating theatre.

The development and execution of safe resection plans for liver tumors requires an assessment of the three-dimensional (3D) relationship between each tumor and the neighboring hepatovascular and biliary structures. At least 40% of the human population is characterized by an unusual anatomical variation of the hepatic arteries or biliary tract [3]. As a result of the continuously increasing complexity of oncological liver resections, the incidence of intraoperative complications related to damage to the biliary ducts with an unusual anatomy increased from <3 to 6% of all postoperative complications in the last decade, underlining the importance of preoperative knowledge of the biliary anatomy [4].

Due to such an increase in the complexity of liver resections in the last decade, more hospitals have started using patient-specific 3D models of the liver anatomy during the preparation of complex procedures, aimed at improving the intraoperative assessment of the liver and facilitating the localization of liver tumors and their vital surrounding structures. Most of these 3D liver models are based on contrast-enhanced CT [5], understandably, due to the easier atomization of CT-based segmentations. In contrast, the 3D models of the liver discussed in this work are explicitly based on dynamic MRI scans with hepatospecific contrast agents. These MRI scans have higher sensitivity than CT for detecting liver malignancies [6, 7], especially those <1 cm. Additionally, they enable visualization of the complete vascular and biliary tree anatomy, together with the malignancy, within one diagnostic scan. Intraoperative biliary tree damage is the only type of surgical complication proven to be directly related to increasing complexity of liver resections (i.e., due to high anatomical variability) [4]. Therefore, integration of patient-specific biliary anatomy into the 3D model, implying the use of 3D models based on MR images with hepatospecific agents, is of essential importance.

The Netherlands Cancer Institute–Antoni van Leeuwenhoek Hospital (NKI-AVL) is a specialized cancer institute where 125 liver tumor resections are performed annually. Here, approximately 40% of the liver tumor resections are classified as major resections based on the Brisbane classification [8] and require the use of a patient-specific anatomy model during preoperative planning as well as during the surgery itself. Considering the lack of a commercially available segmentation method for obtaining diagnostic liver MRI images, outsourcing of the model production is the only option for generating of the model, but this constitutes an unsustainable financial burden for the surgical oncology department. To address this challenge, a method of automatically generating the patient-specific model from diagnostic MRI images was developed in-house and, to date, has been used in >335 cases (Fig. 1). In this

Eur Surg Res 2020;61:143–152
DOI: 10.1159/000513335

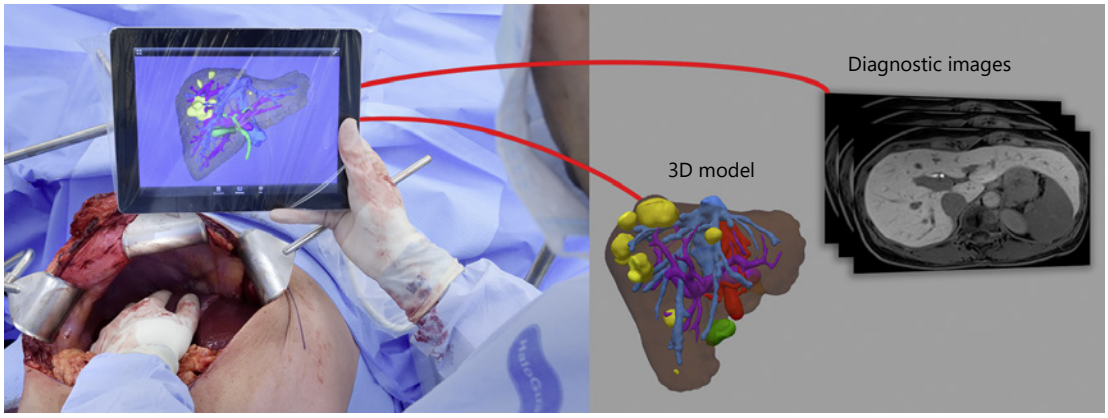

Fig. 1. An illustration of interactive intraoperative viewing of a patient-specific 3D model of the liver and diagnostic imaging with help of a touchscreen tablet. To guarantee sterility of the interaction, the tablet was enclosed in a sterile cover.

Table 1. Parameters for multiscale vessel-enhancing filtering of the liver vessels, hepatic artery, and biliary ducts from a 4D MRI acquisition with a hepatobiliary-specific contrast agent

Vessel type	Scales, *n*	Min and max scale	Contrast	Phase of the MRI dataset	α/β/γ
Biliary ducts	5	1 and 5 mm	bright	hepatobiliary	0.5/0.5/100
Hepatic artery	5	1 and 5 mm	bright	early arterial	0.5/0.5/100
Portal vein	5	3 and 8 mm	dark	late arterial	0.5/0.5/100
	5	3 and 8 mm	bright*	hepatobiliary	0.5/0.5/100
Hepatic vein	5	3 and 8 mm	dark	hepatobiliary	0.5/0.5/100

* Alternative segmentation option.

paper, a stepwise description of the method, together with its pitfalls and the possibility of subsequently integrating the interactive 3D models into the sterile surgical environment, is provided.

Methods

Imaging Modality

Gd-EOB-DTPA-enhanced [9] (Primovist® in Europe, Eovist® in the USA, Bayer Healthcare, Germany) 3D FFE-mDixon multiphase MRI scans were used for automated liver segmentation and the subsequent creation of patient-specific 3D models. Gd-EOB-DTPA is a gadolinium-based hepatospecific agent [9, 10], actively taken up by hepatocytes and excreted into the bile. It therefore allows for the dual benefit of early dynamic imaging of the vascular distribution and delayed hepatobiliary phase imaging [11, 12] to obtain additional data (i.e., currently the only diagnostic imaging modality allowing for such a combination). Image acquisition involves 5 consecutive phases acquired during early enhancement of the contrast agent (i.e., precontrast, early arterial [approx. 10 s post-injection], late arterial [approx. 30 s post-injection], portal venous [approx. 1 min post-injection], and intermediate phase [approx. 3 min post-injection]) and 1 late phase showing hepatospecific filtration of the agent 20 min post-injection. Each phase is acquired with a 3D T1-weighted FFE-mDixon sequence, with a 12-s breath-hold scan in expiration, and a voxel size of 1.0 × 1.0 × 1.5 mm. The single breath-hold scan with an acquisition duration of <17 s is necessary to minimize breathing motion artefacts in the images.

Liver Segmentation Method

In previous work by our group [13], a segmentation algorithm for multiphase MRI scanning of the liver was developed and incorporated into a custom "Liver segmentation pilot" extension of the 3D slicer [14], and is available to download at the GitHub opensource platform [15]. This extension allows for fully automated extraction of the liver contour from a multiphase image and involves 3 dynamic MRI phases using 4D k-means clustering and geodesic contour refinement. These MRI phases are the early arterial, portal venous, and hepatobiliary phases of dynamic MRI acquisition. If no 4D dataset is available, liver contour segmentation on the late-phase image only can also be performed.

After automatic cropping of the 4D MRI dataset, 4D k-means clustering (or 3D clustering on the late-phase image) is used to estimate the position and shape of the liver contour, which is subsequently automatically refined using morphological operations and geodesic active contours, resulting in the final organ contour.

The hepatic and portal vasculature, hepatic artery, and biliary ducts are segmented from various phases of the scan according to their size (i.e., the minimum and maximum vessel diameter) and characteristic contrast (i.e., positive or negative contrast), using a Hessian-based vessel-enhancing filter. This step can be performed using a readily available VMTK extension of the 3D slicer or the "Vesselness calculation" module of the "Liver segmentation pilot" extension described in our previous work [13], using the segmentation parameters listed in Table 1 (for more details on the effect that various vesselness parameters may have on the results of the segmentation, please consult [13] and [16]).

Lastly, tumor contours are manually added to the segmentation using the Editor segmentation module of the 3D slicer [12].

iPad Integration of the Model

To enable intraoperative interaction and viewing of the 3D models on an iPad, the models were imported into a free 3D visualization app for IOS (KiwiViewer v2.0 [17]). Standardized color-coding of all anatomical structures of the model and 3D scene creation was achieved using the publicly available "KiwiViewer Scene File" script in ParaView v4.1 (Kitware Inc., Clifton Park, NY, USA) [18] (online suppl. Appendix 1;for all online suppl. material, see www.karger.com/doi/10.1159/000513335). This application provides the surgeon with easily accessible viewing of the 3D scene, with options to position, rotate, and zoom in on the model according to their own judgment during surgery. Additionally, interactive viewing of selected diagnostic scans was enabled by the OsiriX HD (Pixmeo SARL, Geneva, Switzerland) DICOM viewing app. During surgery, the tablet was covered in a sterile cover (Nilymed, Israel) (Fig. 1). It should be noted that specific coloring of the model should be determined for every hospital individually, taking into consideration the surgeon's preference, the lighting of the operating field, and the dominant colors within the sterile field.

Required Staff and Accuracy Validation of the Models

Segmentation of patient-specific models is performed by technical-medical staff at our hospital (i.e., a research assistant, technician physician, or radiologic technologist) at the request of the hepatobiliary surgeon. The main reasons for requesting a 3D model are a high number of liver tumors, centrally located liver tumors, and vanished lesions.

Considering the absence of the CE-marking on the in-house developed software, before each use of the interactive model during surgery, segmentation accuracy is inspected by the technical-medical staff and the segmented structures are discussed with the surgeon. The final segmentation is uploaded on a tablet. In total, 15–30 min are required for complete segmentation (vessels, biliary ducts, tumors, and liver contour) and loading of the 3D model, as well as to load any available diagnostic scans (MRI and CT) onto the touchscreen tablet. The amount of time required depends on the number of lesions and scan quality and is indicated per case in Figure 2.

Discussion

A general advantage of using interactive 3D models of patient anatomy during preparation and surgical resection is that it enables a more intuitive and preoperative assessment of the relationship between tumors and critical vascular or biliary anatomy than conventional imaging can [19]. These 3D models facilitate easier perception of the patient's anatomy in 3D

Eur Surg Res 2020;61:143–152
DOI: 10.1159/000513335

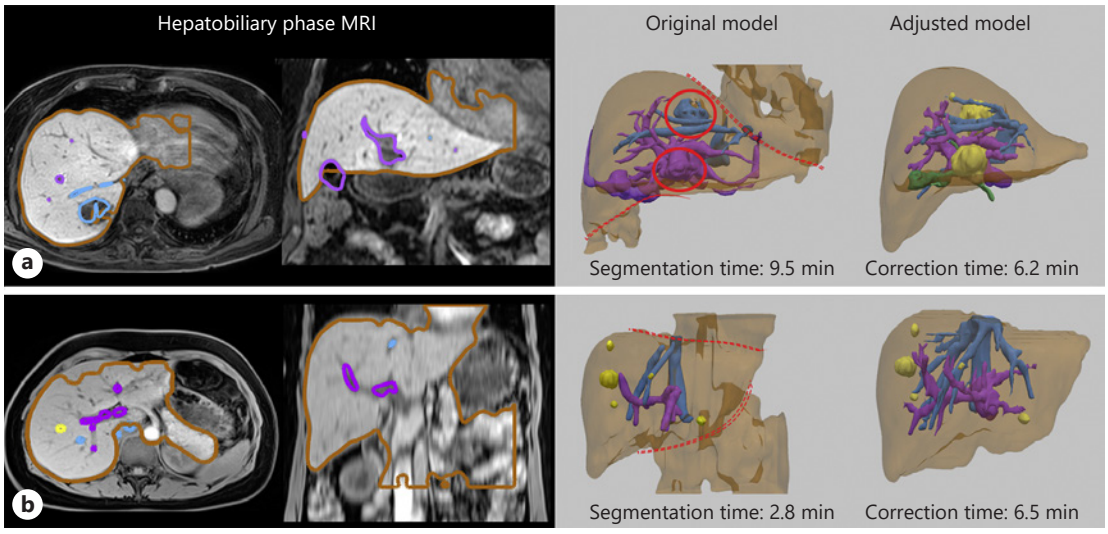

Fig. 2. An illustration of 2 patient-specific models of the liver anatomy that can be created using MRI data that is affected by motion artefacts (**a**) or poor reconstructed resolution (**b**). Both figures contain axial and coronal views (top), together with 3D models before and after manual changes (bottom). **a** 3D model of a patient showing 3 metastases of an adenocarcinoma of the ileum. The 2 large lesions formed a part of the vessel segmentation, which necessitated manual corrections. Additionally, inclusion of the heart in the liver contour required adjustments. **a** 3D model of a patient with 5 colorectal liver metastases. The diagnostic scan was acquired on a 1.2 × 1.2 × 3.0 voxel grid, which hampered extraction of the peripheral vasculature.

(vs. 2D slices) and easier discussion of the resection plan and decision-making by surgeons prior to and during the resection [20]. Three types of clinical cases are expected to derive the highest clinical benefit from the use of the 3D models, namely, patients with (i) vanished lesions or multiple lesions scattered over the organ, (ii) centrally located lesions (Fig. 2a, 3a), and (iii) unusual arterial or biliary tract anatomy (Fig. 3a). In these patient groups, use of the 3D model either helps to avoid permanent morbidity due to unintentional damage to critical liver anatomy (iii above), or facilitates a faster and more radical tumor resection being performed (i and ii above).

Figure 3a illustrates a 3D model of a patient with an intrahepatic cholangiocarcinoma and a large centrally located tumor (a diameter of approx. 4 cm), involving segments I–IVa. The tumor was very close to the middle and left hepatic veins, which required an extended left hemihepatectomy. In addition to the complexity of the case due to this proximity, the patient had a rare variation of the right posterior biliary duct which originated from the left hepatic duct. If surgical resection of this case had been planned without knowledge or consideration of the aberrant biliary anatomy, permanent damage would have occurred which would compromise the biliary drainage of the right liver. We were able to identify and preserve the aberrant right bile duct. Therefore, in this clinical case, the aberrant biliary anatomy affected the surgical decisions, and the use of the 3D model plausibly helped to avoid permanent morbidity of the patient.

Another clinically challenging example is illustrated in Figure 3b. This patient had a primary rectal carcinoma with bilobar spreading of 12 hepatic metastases. After neoadjuvant chemotherapy, all lesions had a diameter varying between 5 and 15 mm, making them difficult to locate with 2D ultrasound. It was decided to perform microwave ablations and wedge resections of all lesions, to ensure sufficient remaining functional liver volume after the procedure. During the surgery, the use of the patient-specific 3D liver model was useful for

Eur Surg Res 2020;61:143–152
DOI: 10.1159/000513335

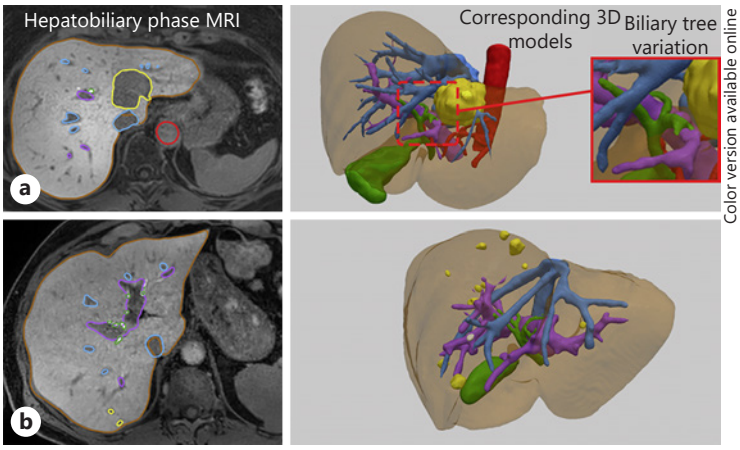

Fig. 3. An illustration of patient-specific models of the liver anatomy that can be created using high-quality MRI data. **a** 3D model of a patient with an intrahepatic cholangiocarcinoma, with a 4-cm lesion, involving segments I–IVa, very close to the left and middle hepatic veins. Here, the model revealed anatomical variation of the biliary tract, with the right posterior segmental duct finding its origin in the left hepatic duct (the aberrant biliary anatomy), which affected surgical resection plan. **b** 3D model of a patient with 13 colorectal liver metastases in segments II and IV–VIII. During surgery, use of the model enabled an easier exploration of all lesions, resulting in an anatomical resection of segments IVb and VII, with additional wedge resections and ablations of all other lesions.

multiple aspects. Firstly, it contributed to a clearly arranged search for all 12 lesions, especially the millimetric ones. Secondly, it reduced the length of the procedure [21], with potential benefits for the patient and the cost of the surgery [22].

The quality of diagnostic MRI scans depends strongly on the physical condition of the patient, required duration of the breath hold, clarity of the instructions throughout the acquisition and contrast timing. These factors affect the quality of the 3D model that can be created automatically, as well as the subsequent workload for model improvement. In Figure 3, we illustrated 2 clinical cases by means of a 3D model extracted from high-quality MRI volumes (e.g., no obvious artefacts, correct contrast timing, and acceptable image resolution). In these cases, complete preparation of the model, including segmentation and image transfer time, typically requires anywhere between 10 and 30 min.

However, when the image quality is affected by motion artefacts or images are acquired with a poor resolution, the following model-degrading effects will appear (Fig. 2, 4). First, motion or poor contrast timing will result in blurring of the dome and base of the liver, ultimately challenging liver-heart separation during the segmentation process. It is not uncommon to observe the "leakage" of the liver mask into the myocardium, when one of these effects is present (Fig. 2a). Simple manual corrections will enable possible liver contour inaccuracies to be removed. Severe motion artefacts (Fig. 4), although seldom observed in our practice, can even distort the visible boundaries of the liver vessels, ultimately jeopardizing the segmentation results. Therefore, it is important to minimize the possible effects of motion (e.g., with parallel imaging techniques). Liver MRI acquisitions are often performed within a single controlled breath-hold. In our hospital, speeding up of MRI data acquisition with parallel imaging techniques (e.g., SENSE) [23] enables us to shorten the total duration of the breath-hold required for MRI phase acquisition, from 20 to 15 s (12 s data-sampling time). This change significantly decreases the frequency of various motion artefacts. Another effect that might appear on scans containing breathing motion is the leakage of vessel masks into

Eur Surg Res 2020;61:143–152
DOI: 10.1159/000513335

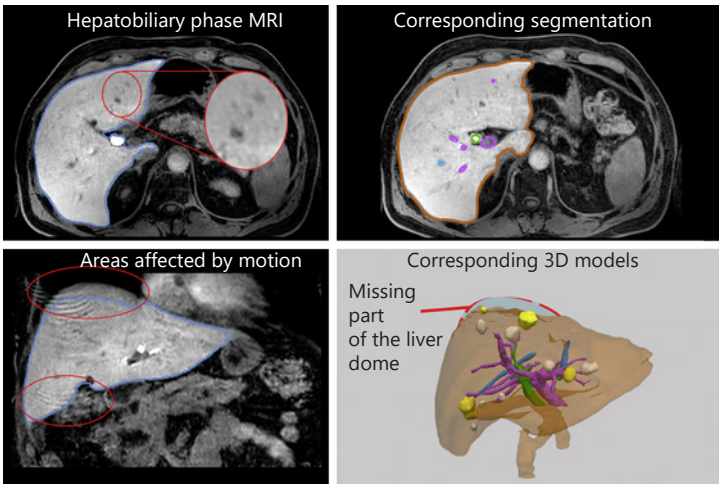

Fig. 4. An illustration of patient-specific models of the liver anatomy that can be created using MRI scan with severe motion artefacts. As a result of the motion, various liver surface boundaries (i.e., the dome of the liver) and the contours of the vessels become blurred, which subsequently affects the extent and accuracy of the segmentation.

the neighboring tumors. This effect is illustrated in Fig. 2a, and it requires the greatest amount of time for making manual corrections.

Second, a parameter that has a strong influence on the quality of the segmentation is the reconstructed image resolution. Unlike on CT, where image resolution is not related to the total scan duration, acquiring higher-resolution MRI data requires a longer sampling time. Therefore, abdominal MRI is standardly acquired on a nonisotropic voxel grid of approximately 1 × 1 × 1.5 mm (Fig. 3). Lower image resolution, especially in the *z*-direction, will have a degrading effect on the extent of the segmentation (Fig. 2b). This is because, although the diameter of the portal and hepatic veins is approximately 7–9 mm where the main vessel branches begin, it rapidly decreases to 2–3 mm at the periphery. Therefore, MRI datasets with z-spacing >3 mm are not suitable for generating patient-specific 3D models of the liver anatomy. In Fig. 2b, one can see the effect of a 2-fold decrease in the image resolution in the longitudinal direction (1.2 × 1.2 × 3 mm, instead of a 1 × 1 × 1.5 mm grid) in the final 3D model. This example represents a less extensive but still clinically acceptable quality of the 3D model.

Another aspect essential for sustainable and financially viable implementation of the 3D models into clinical practice is the presence of dedicated technical support (e.g., by a research assistant, technician physician, or radiologic technologist), which is seldom present in surgical departments outside dedicated medical centers. In contrast, radiotherapy departments have an extensive technical support team responsible for critical anatomy segmentation and radiation treatment planning. Within radiology and nuclear medicine departments, dedicated technical support for image processing became more accepted for patient-specific volumetric analyses and critical anatomy segmentation prior to complicated interventions (e.g., radioembolization and CT-guided ablations). Additionally, these teams take on other technical support tasks, thereby speeding up the implementation of innovative techniques into the clinical practice. While innovative techniques are emerging extensively in the operating theatre, the need for such technological support teams may become more obvious for surgical departments.

This paper focuses on the implementation of the segmentation workflow based on multiphase liver MRI with a hepatospecific contrast agent, Gd-EOB-DTPA. As mentioned above,

Eur Surg Res 2020;61:143–152
DOI: 10.1159/000513335

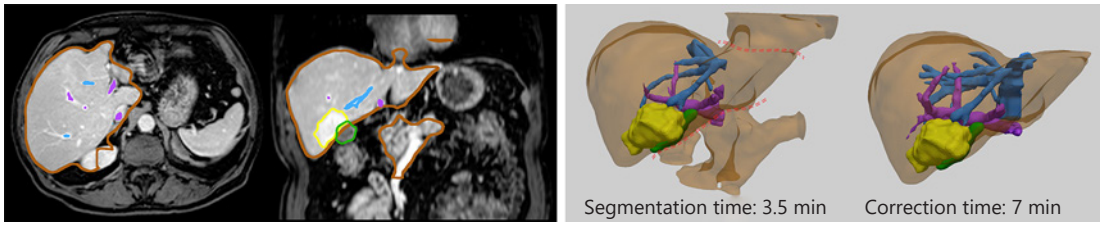

Fig. 5. An illustration of patient-specific models of the liver anatomy that can be created using MRI scanning with an extracellular Gd-based MRI contrast agent.

this contrast agent was selected due to its good tumor detectability and unique late pharmacokinetics (e.g., hepatobiliary phase). However, despite these advantages, a significant number of patients scheduled for liver resection will have MRI image acquisition using alternative extracellular contrast agents like Gd-DTPA and Gd-DOTA. It will still be possible to generate a patient-specific 3D model of liver anatomy using a dynamic scan with an extracellular contrast (Fig. 5). The use of alternative imaging sequences can hamper the extent and accuracy of the segmentation. It is not expected, however, that vessel segmentation will be affected. Nevertheless, minor-to-strong leakage of the liver contour into the heart or vena cava region is likely to occur and will require manual correction. This will increase the total segmentation time and should be taken into consideration during clinical implementation of the technique. At the same time, if image segmentation is performed using a diagnostic MRI with an extracellular contrast agent, it will no longer be possible to add a patient-specific model of the hepatobiliary tree to the 3D model according to the method described in this paper. Hospitals that use magnetic resonance cholangiopancreatography (MRCP) during standard presurgical workup of liver patients may consider using these data for visualization of the hepatobiliary anatomy [24]. However, if the 3D model is used to guide surgical resections, integration of MRCP-based biliary tree segmentations should be accompanied by extra precautions, due to the relatively pronounced nonisometric geometric distortions on MRCP images.

The use of patient-specific 3D models for liver surgery is not novel. Several companies and research groups have already developed commercially or freely available software, although these are mainly for CT-based liver models (e.g., MeVis Medical Solutions AG, Germany, and Visible Patient™, IRCAD, Strasbourg, France) [25, 26]. After the introduction of Primovist in clinics in Europe, studies have shown that gadoxetic acid-enhanced MRI is significantly better for detecting liver lesions than conventional MRI or contrast-enhanced CT [27, 28]. Nowadays, diagnostics with gadoxetic acid-enhanced MRI is a part of standard imaging protocols for patients planned for surgery, and neoadjuvant chemotherapy. For patients with liver malignancies, these specific Primovist scans will be used for treatment planning as well. However, there are no automatic segmentation method to generate MRI-based models of the complete liver anatomy. Only a few groups have tried to address this challenge [29], but there is no readily available method that can be used to generate 3D liver models based on these MRI scans. Therefore, the novelty and importance of this work is the segmentation pipeline and its clinical implementation in the surgical workflow, which is now available for introducing into other surgical departments. Additionally, the publicly available source code is compatible with open source imaging software and libraries (e.g., ITK and VTK), thus allowing for simple implementation in other applications.

Interactive visualization of patient-specific anatomical 3D models on touchscreen tablets is already used in surgery for a wide range of innovative pre- and intraoperative purposes [30, 31]. However, in most cases, the segmentation and the generation of the 3D models is

outsourced to commercial parties. The preoperative creation of 3D models described in this study shows a quality of segmentation and visualization equivalent to those created by outsourcing; however, developing and maintaining this workflow will prove to be more financially viable.

Acknowledgements

The authors thank Bas Pouw for helping in setting up the clinical implementation of this work.

Conflict of Interest Statement

The authors have no conflicts of interest to declare.

Funding Sources

We gratefully acknowledge support for this work in the form of a research grant ("Three-dimensional imaging and navigation during surgery for colorectal liver metastases") from the Breuning ten Cate Foundation.

Author Contributions

Conceptualization and study design: O.V.I., J.N.S., J.N., K.F.D.K., L.t.B., E.J.R., and T.J.M.R. Investigation and data collection: O.V.I., J.N.S., N.F.M.K., T.J.M.R., and K.F.D.K. Data analyses: O.V.I., J.N.S., and K.F.D.K. Funding: K.F.D.K. and T.J.M.R. All authors contributed to the writing and review of the manuscript.

Data and Software Availability

The data and software used for this study are available from the corresponding author (O.V.I.) upon reasonable request and via collaborative investigations.

References

1 Chua TC, Saxena A, Liauw W, Kokandi A, Morris DL. Systematic review of randomized and nonrandomized trials of the clinical response and outcomes of neoadjuvant systemic chemotherapy for resectable colorectal liver metastases. Ann Surg Oncol. 2010 Feb;17(2):492–501.
2 Catalano OA, Singh AH, Uppot RN, Hahn PF, Ferrone CR, Sahani DV. Vascular and biliary variants in the liver: implications for liver surgery. Radiographics. 2008 Mar-Apr;28(2):359–78.
3 Puente SG, Bannura GC. Radiological anatomy of the biliary tract: variations and congenital abnormalities. World J Surg. 1983 Mar;7(2):271–6.
4 Zimmitti G, Roses RE, Andreou A, Shindoh J, Curley SA, Aloia TA, et al. Greater complexity of liver surgery is not associated with an increased incidence of liver-related complications except for bile leak: an experience with 2,628 consecutive resections. J Gastrointest Surg. 2013 Jan;17(1):57–64.
5 Mise Y, Hasegawa K, Satou S, Shindoh J, Miki K, Akamatsu N, et al. How Has Virtual Hepatectomy Changed the Practice of Liver Surgery? Experience of 1194 Virtual Hepatectomy before Liver Resection and Living Donor Liver Transplantation. Ann Surg. 2018 Jul;268(1):127–33.
6 Hammerstingl R, Huppertz A, Breuer J, Balzer T, Blakeborough A, Carter R, et al.; European EOB-study group. Diagnostic efficacy of gadoxetic acid (Primovist)-enhanced MRI and spiral CT for a therapeutic strategy: comparison with intraoperative and histopathologic findings in focal liver lesions. Eur Radiol. 2008 Mar;18(3):457–67.
7 Böttcher J, Hansch A, Pfeil A, Schmidt P, Malich A, Schneeweiss A, et al. Detection and classification of different liver lesions: comparison of Gd-EOB-DTPA-enhanced MRI versus multiphasic spiral CT in a clinical single centre investigation. Eur J Radiol. 2013 Nov;82(11):1860–9.
8 Strasberg SM. Nomenclature of hepatic anatomy and resections: a review of the Brisbane 2000 system. J Hepatobiliary Pancreat Surg. 2005;12(5):351–5.

9 Reimer P, Schneider G, Schima W. Hepatobiliary contrast agents for contrast-enhanced MRI of the liver: properties, clinical development and applications. Eur Radiol. 2004 Apr;14(4):559–78.
10 Seale MK, Catalano OA, Saini S, Hahn PF, Sahani DV. Hepatobiliary-specific MR contrast agents: role in imaging the liver and biliary tree. Radiographics. 2009 Oct;29(6):1725–48.
11 Yeh BM, Liu PS, Soto JA, Corvera CA, Hussain HK. MR imaging and CT of the biliary tract. Radiographics. 2009 Oct;29(6):1669–88.
12 Hennedige TP, Neo WT, Venkatesh SK. Imaging of malignancies of the biliary tract- an update. Cancer Imaging. 2014;14(1):14.
13 Ivashchenko OV, Rijkhorst EJ, Ter Beek LC, Hoetjes NJ, Pouw B, Nijkamp J, et al. A workflow for automated segmentation of the liver surface, hepatic vasculature and biliary tree anatomy from multiphase MR images. Magn Reson Imaging. 2020 May;68(May):53–65.
14 Pieper S, Lorensen B, Schroeder W, Kikinis R. The NA-MIC Kit: ITK, VTK, Pipelines, Grids and 3D Slicer as An Open Platform for the Medical Image Computing Community. 3rd IEEE International Symposium on Biomedical Imaging: Macro to Nano. 2006; pp 698–701.
15 Ivashchenko O, Rijkhorst E. GitHub repository [Internet]. Liver segmentation Pilot. 2018. Available from: https://github.com/oivashchenko/liver-segmentation
16 Frangi AF, Niessen WJ, Vincken KL. Viergever MA. Multiscale vessel enhancement filtering. In: Wells WM, Colchester A, Delp SL, editors. Medical Image Computing and Computer-Assisted Intervention. Berlin: Springer; 1998. pp. 130–7.
17 Kitware Inc. [Internet] KiwiViewer [cited 2019 Sep 1]. Available from: http://www.kiwiviewer.org/
18 Kitware Inc. [Internet] ParaView [cited 2019 Sep 1]. Available from: https://www.paraview.org/
19 Beermann J, Tetzlaff R, Bruckner T, Schöebinger M, Müller-Stich BP, Gutt CN, et al. Three-dimensional visualisation improves understanding of surgical liver anatomy. Med Educ. 2010 Sep;44(9):936–40.
20 Hansen C, Zidowitz S, Preim B, Oldhafer KJ, Hahn HK. Impact of model-based risk analysis for liver surgery planning. Int J Comput Assist Radiol Surg. 2014;9:473–80.
21 Yeo CT, MacDonald A, Ungi T, Lasso A, Jalink D, Zevin B, et al. Utility of 3D Reconstruction of 2D Liver Computed Tomography/Magnetic Resonance Images as a Surgical Planning Tool for Residents in Liver Resection Surgery. J Surg Educ. 2018;75(3):792–7.
22 Ballard DH, Mills P, Duszak R, Weisman JA, Rybicki FJ, Woodard PK. Medical 3D Printing Cost-Savings in Orthopedic and Maxillofacial Surgery: Cost Analysis of Operating Room Time Saved with 3D Printed Anatomic Models and Surgical Guides. Acad Radiol. 2020;27(8):1103–13.
23 Katscher U, Börnert P. Parallel RF transmission in MRI. NMR Biomed. 2006 May;19(3):393–400.
24 Gloger O, Bülow R, Tönnies K, Völzke H. Automatic gallbladder segmentation using combined 2D and 3D shape features to perform volumetric analysis in native and secretin-enhanced MRCP sequences. MAGMA. 2018 Jun;31(3):383–97.
25 Kohlmann P, Boskamp T, Köhn A, Rieder C, Schenk A, Link F, et al, editors. Remote visualization techniques for medical imaging research and image-guided procedures. In: Visualization in Medicine and Life Sciences III. New York (NY): Springer; 2016. pp. 133–54.
26 Ntourakis D, Memeo R, Soler L, Marescaux J, Mutter D, Pessaux P. Augmented Reality Guidance for the Resection of Missing Colorectal Liver Metastases: An Initial Experience. World J Surg. 2016 Feb;40(2):419–26.
27 Jiang HY, Chen J, Xia CC, Cao LK, Duan T, Song B. Noninvasive imaging of hepatocellular carcinoma: from diagnosis to prognosis. World J Gastroenterol. 2018 Jun;24(22):2348–62.
28 Zech CJ, Korpraphong P, Huppertz A, Denecke T, Kim MJ, Tanomkiat W, et al.; VALUE study group. Randomized multicentre trial of gadoxetic acid-enhanced MRI versus conventional MRI or CT in the staging of colorectal cancer liver metastases. Br J Surg. 2014 May;101(6):613–21.
29 Liu M, Vanguri R, Mutasa S, Ha R, Liu YC, Button T, et al. Channel width optimized neural networks for liver and vessel segmentation in liver iron quantification. Comput Biol Med. 2020 Jul;122:103798.
30 Mobasheri MH, Johnston M, Syed UM, King D, Darzi A. The uses of smartphones and tablet devices in surgery: A systematic review of the literature. Surgery. 2015 Nov;158(5):1352–71.
31 Matsuyama R, Mori R, Taniguchi K, Nojiri K, Hiratani S, Takeda K, et al. IPAD guided right hemihepatectomy with a new application designed specifically for navigation surgery: initially clinical experience for perihilar cholangiocarcinoma. HPB (Oxford). 2014;16:289–90.